



Review

Review of Residual Stress Impingement Methods to Mitigate Environmental Fracture Susceptibility

Matthew E. McMahon

Naval Surface Warfare Center, Carderock Division, Bethesda, MD 20817, USA; matthew.e.mcmahon1@navy.mil

Abstract: Environmental cracking- and fatigue-related failures threaten all major industries and, to combat such degradation, numerous residual stress impingement (RSI) methods have been developed with varying levels of efficacy and ease of use. Some of the most commonly used RSI methods, such as shot peening, laser shock peening, and low plasticity burnishing, as well as new methods, such as ultrasonic nanocrystal surface modification, are reviewed in the context of corrosion, corrosion fatigue, and environmental cracking mitigation. The successes and limitations of these treatments are discussed, with a focus on their efficacy against these three damage modes based on the available literature. Case studies are reviewed that demonstrate how these treatments have been adopted and advanced by industry, and application-specific research efforts are explored with a focus on future opportunities. Research is identified that illustrates how the utility of these surface treatments may vary between alloy systems, and where the benefits must be weighed against the risks to a component's service performance.

Keywords: residual stress; stress corrosion; corrosion fatigue; laser peening; low plasticity burnishing; shot peening



Citation: McMahon, M.E. Review of Residual Stress Impingement Methods to Mitigate Environmental Fracture Susceptibility. *Corros. Mater. Degrad.* **2021**, *2*, 582–602.
<https://doi.org/10.3390/cmd2040031>

Academic Editor: Richard Barker

Received: 2 June 2021

Accepted: 8 October 2021

Published: 20 October 2021

Publisher's Note: MDPI stays neutral with regard to jurisdictional claims in published maps and institutional affiliations.



Copyright: © 2021 by the author. Licensee MDPI, Basel, Switzerland. This article is an open access article distributed under the terms and conditions of the Creative Commons Attribution (CC BY) license (<https://creativecommons.org/licenses/by/4.0/>).

1. Introduction

Metallic components undergo stress due to externally applied forces and/or internal residual forces, with the latter often originating from thermally induced deformation during production or from the forming and machining processes. Over time in service, these stresses may act in concert with the surrounding environment, component geometry, surface defects, corrosion, and more to induce subcritical damage in the form of fatigue, corrosion fatigue, or environmentally assisted cracking (EAC). These phenomena affect the majority of alloys under the right conditions, and all require a minimum stress intensity (K)/stress intensity amplitude (ΔK) condition to initiate and propagate [1]. The ubiquity of these mechanisms across industries warrants their mitigation, which can be achieved by inserting technologies that reduce the likelihood that those minimum requirements will be met. Applicable technologies for newer construction include coatings, cladding, corrosion protection, and surface treatments, such as residual stress impingement (RSI). These proactive sustainment efforts can help to avoid unexpected costs, structural deficiencies, failures, and loss of life. As vehicles and parts age, the likelihood of significant defect formation due to damage, use, and environmental effects increases, which in turn decreases the required stress input needed to achieve crack initiation and growth [2]. Thus, the aging infrastructure that exists within many industries today increasingly requires proactive maintenance to mitigate aggressive environmentally induced damage. For these critical but aged components, RSI technologies are a primary candidate to achieve life extension.

RSI methods impart compressive residual stresses that reduce $K/\Delta K$ locally and combat crack initiation/propagation. These techniques are crucial for the preventative maintenance of new components, as well as for the sustainment of aging vehicles and parts. Residual stress impingement techniques, such as shot peening (SP), have been applied

to metal surfaces for fatigue life improvement for over 60 years [3]. More recently, new advancements have been introduced, such as laser shock peening (LSP), low plasticity burnishing (LPB), and ultrasonic nanocrystal surface modification (UNSM), to name some common examples. These new methods have arisen to improve treatment consistency, residual stress penetration depth and stability, and surface finish, as well as other performance attributes. Reviews exist covering a range of RSI methods and their benefits, as well as expressing related concerns. McClung addressed residual stress stability and the impact of various residual stress impingement methods on fatigue [3]. Schultze and Lu have published thorough reviews of various RSI methods and their effects on the mechanical performance of materials [4,5]. Additionally, method-specific reviews exist on LSP due to this technique's rising significance. Montross reviewed the fatigue improvements achieved through LSP treatment [6], and Sundar recently reviewed the development and modern applications of LSP [7]. Sano reviewed 25 years of LSP development efforts, with a specific focus on steel applications in the nuclear power industry [8]. Priyadarsini reviewed the most common burnishing-related RSI methods (ball, roller, and LPB), and compared them against one another in residual stress penetration and stability, as well as the ability to improve fatigue, corrosion fatigue, fretting, and environmental cracking [9]. These reviews and others provide considerable insight into the many RSI methods and common applications. However, interest has steadily increased in applying RSI methods to address environmental cracking concerns, such as surface corrosion and related defect formation, corrosion fatigue, and EAC. No review currently exists that evaluates and compares the leading RSI methods and their ability to mitigate corrosion, corrosion fatigue, and EAC susceptibility, which the present review will address.

This review will summarize the state of the art in the use of RSI on alloys of varying hardness for the purposes of (1) corrosion minimization, (2) fatigue/corrosion fatigue mitigation, and (3) the mitigation of EAC. The literature review will focus on RSI treatment on wrought and cast alloys. The use of RSI in welded alloys will also be briefly reviewed, due to the common sensitization and EAC concerns that arise in steel. Recent advances in the use of these surface treatments will be discussed, and the remaining knowledge gaps will be identified. Lastly, case studies will be explored that detail the unique application and advancement of RSI in various industrial sectors for the purpose of mitigating corrosion, corrosion fatigue, and EAC.

2. Research Methods

This literature review focused on publications released in the last 15 years (2006–2021) concerning SP, UNSM, LSP, and LPB and related effects on corrosion, corrosion fatigue, and EAC in wrought and cast alloys evaluated at temperatures below 200 °C. Notable works having greater age were also included, when useful. Scopus indices were utilized, as well as direct searches within individual journal databases. Search results were evaluated based on the above criteria, via titles, abstracts, and key words, to select the most applicable publications, after which the selected publications were evaluated in greater detail. The applicable works were selected from the total search results for each "Main Topic" plus "Key Word" combination (Table 1), based on the quality of the research methods, the clarity of the findings, and the applicability of the work based on this review's evaluation criteria ($T < 200$ °C, wrought and cast alloys, a focus on corrosion/EAC/corrosion fatigue). The literature commonly evaluated RSI treatments on alloys with weldments, coatings, or other customizations that made general trends more difficult to verify, and so these works were discarded from consideration. The quantity of results from the Scopus searches during the publication period of 2006–2021 demonstrate the quantity of research focused on environmental degradation and on these RSI methods, and the magnitude of efforts that have been devoted to each (Table 1).

Table 1. Scopus Index Findings and Additional Consulted Works.

Search Criteria: Main Topics	Search Criteria: Key Words	Total Results	Applicable Works
Shot Peening	Corrosion	592	57
	Corrosion Fatigue	75	20
	Cracking	217	17
Ultrasonic Nanocrystal Surface Modification	Corrosion	31	6
	Fatigue	50	28
	Cracking	10	1
Laser Shock Peening	Corrosion	174	38
	Corrosion Fatigue	19	5
	Cracking	57	11
Burnishing	Corrosion	168	24
	Corrosion Fatigue	24	9
	Cracking	34	7
Total		1451	223

The literature documents the effects of RSI on a wide variety of alloys, covering a range of strengths, hardness, and passivity. For the sake of comparison, these alloys will be grouped according to surface hardness, since this characteristic commonly affects how an RSI treatment will impact a given alloy via compressive residual stress magnitude and depth, surface roughness, and grain refinement. Where hardness was not explicitly stated in the literature, online material databases were utilized to determine reasonable hardness values. These groupings are demonstrated in Table 2 for several of the alloys considered within this review.

Table 2. Alloy Groupings Based on Hardness (Prior to RSI Treatment).

Hardness Level	Hardness Range (According to Vickers Hardness)	Alloys
Low	10–100	AZ31B, 6082, 5083, Brass 260/280
Medium	100–200	7075, 7050, 2024, 6061, AISI 430 steel
High	200+	C35 steel, 304 SS, 316 SS, 300M, 36NiCrMo, 42CrMoV, 12Cr Steel, Ferrium S53

3. Introduction to Residual Stress Impingement Methods

In general, RSI methods aim to impart compressive residual stresses into a metal surface that will offset external applied, or existing residual, tensile stresses. By reducing these stresses, the crack initiation and/or propagation rate may be decreased due to reduced stress intensity being present at the site of a small defect, or at a crack tip. These compressive residual stresses have a maximum effect while the defect remains within the compressively stressed material layer, and so the effective penetration depth achieved by a given RSI method is key. The most commonly utilized RSI treatments all have advantages as well as drawbacks that affect the final state of the alloy surface microstructure, the magnitude and depth of the imparted compressive stress, the resultant surface finish, and the efficiency of its application. Selected treatment methods will be briefly summarized.

Shot peening is one of the oldest RSI methods that are still commonly utilized today and consists of firing high-hardness shot (often glass, metal, or ceramic, depending on the target and goal) at a metal surface to impart compressive residual stress (CRS). This process is demonstrated schematically in Figure 1A. The SP process is controlled by the Almen intensity and coverage, where the Almen intensity reflects the effect of spot size, shot hardness, speed, flow rate, and impact angle [10]. An advantage of SP is its relative ease of application compared to some other methods, and the deep knowledge base associated with the history of its use [11]. One downside of the method is that, due to the aggressive bombardment of a surface with shot, the process parameters must be carefully controlled

to achieve the desired surface roughness and consistent surface coverage, which is not as uniform as with other methods [12]. The overtreatment of a surface during SP may result in brittle cracking in the deformed surface layer, folds that may conceal defects, and even embedded shot, all of which could aggravate corrosion or crack formation [13]. The impact of shot on the alloy surface leaves dimples that form a gradient of compressive residual stress that commonly reaches 0.25–0.50 mm in depth [14,15]. The ultrasonic nanocrystal surface modification (UNSM) process uses a tungsten carbide-tipped applicator that is pressed down onto the alloy surface with a specific load and vertically vibrates at an ultrasonic frequency while moving systematically around the alloy surface [16]. The UNSM process is schematically illustrated in Figure 1B. This treatment is computer-directed; therefore, a uniform surface coverage is achieved that results in a low hardness increase and a low surface roughness increase in a variety of alloys [16]. UNSM commonly forms a nanocrystalline grain structure below the alloy surface, and the CRS depth tends to be similar to that seen with SP [16].

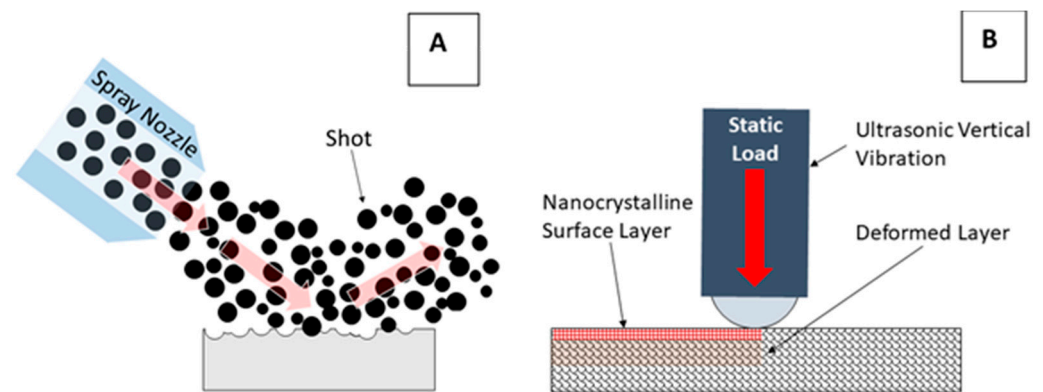


Figure 1. Schematic representations of (A) the shot peening process, and (B) the ultrasonic nanocrystal surface modification process.

Laser shock peening utilizes laser energy bombardment to impact a surface water layer and create plasma pulses through an underlying material, which drives in the CRS [6,15]. The LSP process is schematically illustrated in Figure 2A. The advantages of LSP include the fact that this process is computer-controlled, and each laser shot is measured and the output energy is recorded, making the process highly traceable and repeatable. The surface coverage is uniform and the CRS depths are consistent. CRS depths typically range from 0.75–1.25 mm when no ablative layer is used (Figure 3) [8]. When an ablative layer is used, the maximum residual stress is similar to that which is achieved without an ablative layer but the maximum penetration depth is reduced; thus, this treatment method is less common [17]. The LSP process is tuned through the laser spot size and power density applied to the alloy surface, as well as the beam overlap, all of which impact the CRS depth and final surface roughness [6,7]. One disadvantage of LSP is that this method must be utilized in controlled settings, and strict control of the surrounding area is required due to the hazard of the laser, which can make LSP one of the more expensive RSI methods to deploy. Overtreatment through LSP occurs through the application of excessive power density, which can actually form tensile stress in the surface layer and can cause melting [18,19]. However, this is easily avoidable through preliminary research on best practices for treating a given alloy type. Lastly, LPB utilizes a hydraulically pressed bearing to apply force to an alloy surface without applying heat or causing significant microstructural deformation (Figure 2B) [20].

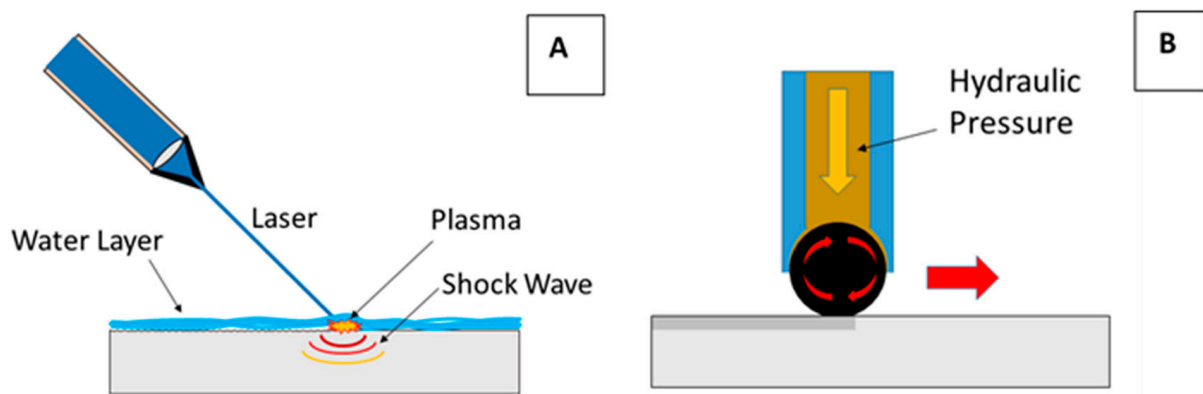


Figure 2. Schematic representations of (A) the laser shock peening treatment process (shown without the damping layer), and (B) the low plasticity burnishing process.

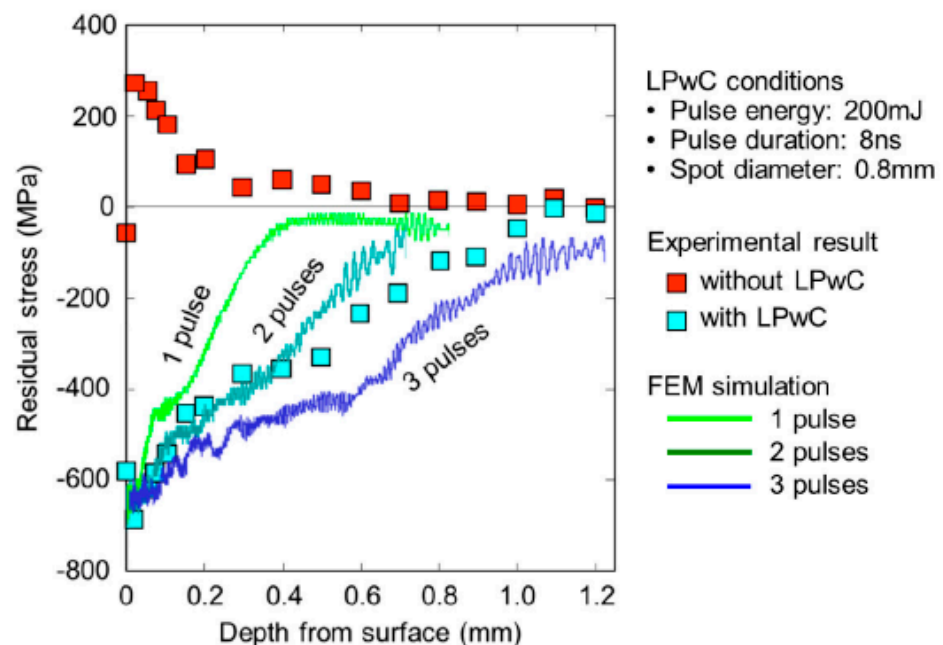


Figure 3. Impact of LSP applied 1–3 times on 316L steel weldments, compared to the residual stress profile without treatment. LPwC—laser peening without ablative coating [8]. Reprinted with permission from [8]. Copyright 2020, Metals Journal in MDPI.

This process induces minimal changes to the alloy surface profile and is proven to impart similarly high magnitude compressive residual stresses as are achieved with LSP, to a depth of roughly 1 mm or greater. An example dataset from Inconel 718 is illustrated in Figure 4, which compares the CRS depth and magnitude achieved by SP, LSP, and LPB [4,21].

Due to the use of a hydraulically loaded ball bearing, this process is best used on open surfaces, where it can easily be utilized in a CNC machine to complement a typical machining process before the part is completed. The benefits and risks of the SP, UNSM, LSP, and LPB processes have varying impacts on the ability to improve corrosion performance in alloys of varying hardness, which will be discussed in the following section.

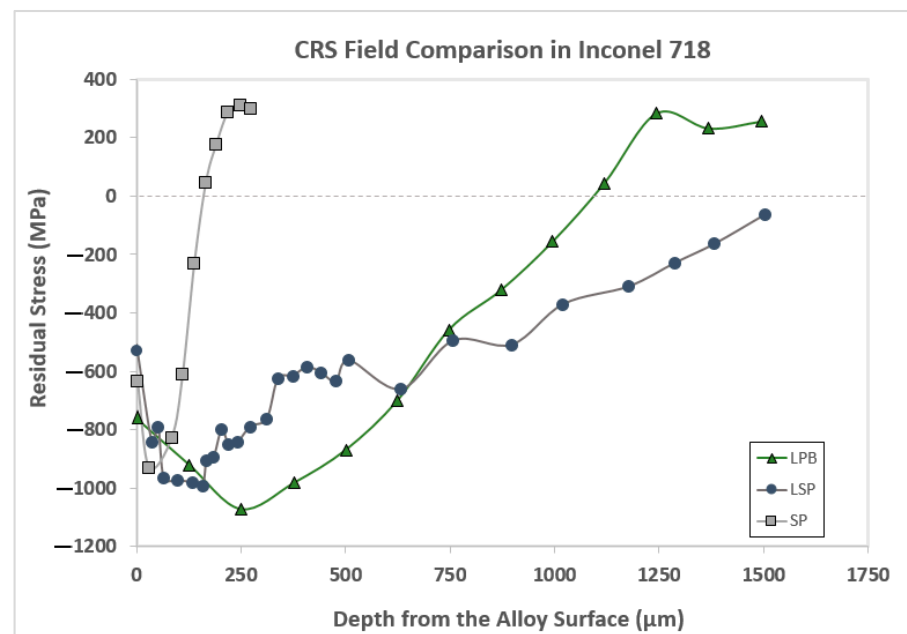


Figure 4. A comparison between the residual stress profiles achieved by SP, LSP, and LPB in Inconel 718 [21]. Reproduced with permission from [21]. Copyright 2003, Journal of Engineering for Gas Turbines and Power on behalf of ASME.

4. Corrosion Minimization

Corrosion is a highly surface-sensitive phenomenon; the effect of surface roughness on corrosion susceptibility is well documented in the literature [22,23]. Residual stress impingement imparts compressive stress into the alloy surface, which can improve corrosion resistance through a combination of work-hardening and grain refinement. However, RSI treatments can also increase the surface topography, which may reduce the benefit of the compressive stress and refined microstructure. Previous works have demonstrated that there is a relationship between the target alloy's passivation mechanism, the surface topography caused by the RSI, and the alloy corrosion resistance [4,24,25].

This relationship is evident when viewed across the hardness spectrum. Considering the effects of SP, firstly on low-hardness alloys, Curtis et al. evaluated shot-peened 2024-T351 (137 HV) via potentiodynamic analysis in 3.5 wt % NaCl and measured a 5-fold increase in the corrosion current density (i_{corr}) compared to the as-polished sample [26]. After 24 h in this solution at an open circuit, the 2024-T351 experienced an increased pitting rate after SP [26]. Similarly, the SP treatment of 7075-T651 (175 HV) increased the alloy's surface roughness from 0.32 μm to 5.81 μm , after which Zupanc and Grum measured a 2.5-factor increase in i_{corr} in 0.1 M NaCl [27]. When evaluating AISI 430 steel (162 HV) after SP, Peltz et al. observed a 10-fold increase in i_{corr} in 0.05 M NaCl, due mainly to the increase in surface roughness from 0.02 μm to 3.18 μm [28]. These examples demonstrate that the RSI-induced roughness in low hardness alloys detrimentally affects the passivity and corrosion resistance.

In the medium-hardness AISI 304 stainless steel (240 HV), Iswanto et al. demonstrated, in intravenous Otsu-Ringer lactate solution, that the pitting rate initially increased by as much as 20 times when SP was conducted for 5 min but decreased as SP was conducted for longer periods of time to achieve better coverage and more plastic deformation across the alloy surface [29]. Treating the 304 SS for 40 min more than doubled the surface hardness to reach 496 HV, and the pitting rate decreased from the as-polished rate of 0.042 mpy to 0.036 mpy [29]. In 316L stainless steel (220 HV), Peyre demonstrated via potentiodynamic analysis that both SP and LSP (8 GW/cm²) achieved similar improvements in the alloy's pitting resistance, and both improved the i_{corr} in 0.5 M NaCl, despite slightly rougher surface finish as well as martensite formation following SP [30]. Interestingly, the open-circuit

potential of the SP-treated 316L was also roughly 100 mV greater than the LSP-treated 316L [30]. Various authors have attributed the LSP-induced improvement in corrosion resistance to slight melting and re-segregation at the alloy surface, such that the high-energy, work-hardened material is less exposed to aggravate corrosion reactions [18,31]. Considering high hardness alloys, Cuifini et al. demonstrated in 300–325 HV super duplex stainless steel that SP treatment resulted in a 3- to 4-fold increase in mass loss through salt fog cabinet exposure [32]. Overall, these findings support the need to understand the alloy's passivity and the dependence on surface morphology before applying RSI, especially when considering techniques such as SP that can cause significant roughness and plastic deformation.

UNSM, despite achieving a more uniform surface finish than SP, can also increase corrosion susceptibility due to the added dislocation density, except in specific circumstances. In the low-hardness AZ31B (60 HV), Hou et al. demonstrated in simulated body fluid (SBF) and 0.1 M NaCl that a 2-fold increase in i_{corr} occurs following UNSM [33]. With Alloy 600 (180 HV), however, UNSM treatment below the critical amplitude was demonstrated by Kim and Kim in 1 wt % NaCl to improve the alloy passivation by creating a reactive nanocrystalline surface with low roughness, which also reduced the pitting susceptibility [34]. However, higher-amplitude treatments increased the surface roughness and created crevice-forming features that promoted aggressive chemistry formation, oxide rupture, and pitting [34]. On 4140 steel, in the annealed (183 HV) and nitrided conditions (450 HV), UNSM treatment decreased the corrosion resistance of the steel in alkaline, neutral, and acidic 3.5 wt % NaCl solutions [35]. In contrast, when Li et al. evaluated UNSM on 304SS (240 HV) in 3.5 wt % NaCl, the data revealed increased nobility and passivity, as well as improved pitting resistance [36]. Closer inspection via transmission electron microscopy (TEM) and surface analysis showed that the UNSM treatment created a cleaner surface with fewer MnS inclusions, and the nanocrystalline surface layer showed better Cr distribution, such that the passive film achieved greater Cr enrichment and improved stability [36]. It is worth noting that Kim evaluated UNSM on 316L (220 HV) in 3.5 wt % NaCl, however, and demonstrated that the improvement in pitting following UNSM depends on the level of sensitization present in the alloy; when sufficiently sensitized, UNSM can actually accelerate the pitting attack [37]. This comparison between 4140, 304SS, and 316SS demonstrates that a strong passivation mechanism in the underlying alloy may assist the RSI to improve corrosion resistance; however, the underlying alloy metallurgy, such as a highly sensitized state, can reverse this trend. In relatively high-hardness Ti-6Al-4V (380 HV), Cao et al. observed increased pitting susceptibility and a 2-fold increase in i_{corr} in SBF after applying UNSM treatment [38]. The disparities between alloys and variable RSI-related corrosion improvement demonstrate the need for a more microstructural-based understanding of why improvements are achieved in some alloys, but not in all.

LSP has a more consistent track record of improving corrosion resistance when not overly applied. In the low hardness 5083-H112 (72 HV), Yang demonstrated that LSP achieved the greatest improvement in the surface corrosion resistance when lower power density was applied for a smoother surface finish, estimating that repassivation in 3.5 wt % NaCl was more stable with less topography [39]. In 6082-T651 (85 HV), LSP evaluations across the power density range of 5.7–15.8 GW/cm² demonstrated that this alloy is less sensitive to power density than 5083 in dilute NaCl, since nearly all LSP treatments within the study achieved a similar reduction in pitting susceptibility, despite a 5-fold increase in surface roughness (0.72 μm to 3.74 μm in the L-direction) [19]. Trdan and Grum later demonstrated that LSP improves the polarization resistance of 6082-T651 by 25-fold, expands the passive electrode voltage region on the potentiodynamic curve, and decreases i_{corr} as much as 10-fold compared to untreated 6082-T651 in 0.6 M NaCl [18]. In 7075-T6 (175 HV), Aravamudhan demonstrated, through potentiodynamic polarization, that LSP reduced i_{corr} by 2–3 times in 3.5 wt % NaCl [40]. Pitting was observed to occur preferentially near the valleys formed during LSP treatment on the 7075-T6, where chemistry could more easily acidify, and the magnitude of valley formation depended on the power density

selection [40]. Considering LPB, Cao demonstrated that LPB reduced mass loss in AZ31B (60 HV) in 5 wt % NaCl over 7 days' immersion, and the corrosion rate was more consistent than that measured on the non-treated samples [41]. The main cause for this improvement was hypothesized to be the smaller grain size and reduction of intermetallic phases near the alloy surface, as well as the smooth surface finish and aligned crystalline orientation generally caused by the LPB, all of which promote corrosion resistance in Mg (but this is likely different in other alloys, especially regarding the effect of grain size) [41]. These collective findings demonstrate that the impact of RSI methods on corrosion susceptibility is largely dependent on alloy, the intensity of surface treatment, and the resulting microstructure. The impact of microstructural changes and surface deformation on the intermetallic presence and oxide stability will also play a significant role in the final corrosion susceptibility. If properly applied, these results demonstrate that specific RSI/alloy combinations and processing could reduce a component's tendency to corrode over a service life, which is an added benefit to well-known CRS-induced fatigue life improvements.

5. Fatigue Mitigation

Prior to evaluating the effects of RSI on the rather complex corrosion fatigue phenomenon, a brief review of mechanical fatigue and known RSI impacts on fatigue is necessary. Fatigue performance depends on a variety of factors including, but not limited to, an alloy's microstructural cleanliness, machining and surface finish, environment, residual stresses, and cyclic load schedule. Deleterious residual stresses may be imparted through manufacturing processes, such as forging, casting, forming, and machining and these stresses will impact fatigue performance, often in complex ways as the stresses redistribute and relax with time in service [3]. These manufacturing stresses, as well as the impact of the cyclic load schedule, have been addressed successfully in a wide range of alloys through the development and utilization of optimized RSI methods. These successes are typically separated by the RSI impact on fatigue initiation, and on fatigue propagation, which will be discussed separately for clarity.

5.1. Fatigue Initiation

Fatigue initiation is considered a stochastic process, one that is believed to be dependent on surface topography/features, stress concentration, and applied stresses, among other factors. RSI methods tend to increase the surface roughness, which can accelerate fatigue crack initiation due to small surface features concentrating the stress. However, the work hardening and surface microstructural refinement achieved by RSI can compete with surface roughness to mitigate initiation, hence the need to understand the optimal RSI settings for specific alloys. The literature in this subject area is mainly focused on SP, due to the long history of this RSI technique in industry, and so these studies will be leveraged for fundamental insights. Gangaraj et al. sought to understand the balance between surface hardening and fatigue initiation in 4340 (339 HV) through modeling, which demonstrated that SP increases the fatigue initiation on the alloy surface even when smaller shot and reduced velocities are utilized to produce less surface roughness [42]. Experimental micro-fatigue crack propagation studies have also provided insight into the impact of fatigue initiation versus fatigue propagation effects following RSI treatment. Wagner [43] evaluated SP and LPB on 2024-T3/T6 (137/142 HV) via interrupted fatigue testing, to measure microcrack initiation and propagation. In the 2024-T3 (360 MPa yield strength, hardening cyclic behavior), SP treatment produced a higher magnitude of residual stress than that achieved in the higher-strength 2024-T6 (420 MPa yield strength, softening cyclic behavior). Crack measurements demonstrated that microcrack formation and growth near the fatigue threshold were greater in -T6 than in -T3; however, the overall difference between these tempers in terms of fatigue life demonstrated that the difference in the effect of the SP was mainly attributable to reduced crack propagation in the higher residual stress field in 2024-T3 [43]. In 300 M steel (746 HV), Bag et al. demonstrated across different SP parameter settings and fractographic analysis that the surface roughness, combined with the CRS

magnitude, dictates whether fatigue initiation will typically occur at the alloy surface or at a subsurface defect [44]. Although they tended to drive initiation at the surface, the SP treatments that resulted in higher surface roughness still achieved longer fatigue life, due to the higher magnitude CRS to reduce crack propagation [44]. Overall, considerable work is still needed to understand the effects of various RSI methods on fatigue crack initiation, especially for newer RSI methods that cause less plastic deformation and surface roughness, for which the literature is sparse. This scarcity is likely due to the strong effects of RSI on fatigue crack propagation, which largely dictates the fatigue life, as well as the ease of evaluating fatigue propagation compared to fatigue initiation.

5.2. Fatigue Propagation

Fatigue propagation is a phenomenon driven by the Paris Law relationship, where the crack growth rate over a single cycle occurs as a function of the stress intensity amplitude, or ΔK . The reduction in effective tensile stress at the fatigue crack tip, which is an input into the ΔK equation, is the means through which RSI treatments may reduce the fatigue crack growth rate (FCGR). Residual stress impingement methods that impart shallow compressive stress fields, such as SP (0.25–0.50 mm depth), are not always effective in mitigating fatigue propagation. Ferreira et al., for example, measured fatigue crack growth in 7475-T7351 (155 HV) with and without SP, and found that the effect of the SP treatment was negligible overall, with only a slight impact measured near the fatigue threshold [14]. These authors also evaluated the impact of the material thickness (4 mm vs. 8 mm) and stress ratio (0.05 vs. 0.4) and found that SP only achieved a slight FCGR reduction when the stress ratio was reduced. Wang et al. evaluated SP-treated Ti-6Al-4V (380 HV) bending beam specimens in fatigue and measured a 34% reduction in the short crack propagation rate from the notch, compared to a reference specimen; however, after a short period of growth, the FCGR was elevated relative to the reference FCGR [45]. RSI methods that impart deeper compressive residual stresses have demonstrated more consistent fatigue crack growth mitigation. In 7075-T7352 (150 HV), Hatamleh et al. demonstrated in fatigue crack propagation tests that LSP reduced FCGR and SP did not, which is in agreement with Ferreira [14,46]. These results suggested that, despite the similar magnitude of compressive residual stress imparted by both processes, there exists a critical depth below which compressive residual stress has a measurable impact on the effective ΔK at the crack front. This depth is especially important at higher stresses, where fatigue initiation is more likely to occur in the alloy subsurface. In 2024-T351 (137 HV), Hu et al. [47] demonstrated that LSP improved fatigue life and FCGR in pre-cracked test specimens through two effects: (1) reducing the resolved tensile stress and ΔK ; and (2) relaxation-induced crack closure to further reduce ΔK . These findings were supported by those of Kashaev et al., who demonstrated the ability to tune the LSP procedure through multiple laser passes, to further reduce FCGR while still avoiding severe microstructural damage [48]. In 6061-T6 (107 HV), Huang et al. demonstrated both experimentally and numerically that LSP increases the fatigue life by decreasing the fatigue crack propagation rate in compact tension test specimens [49]. Lastly, Prevey et al. observed that LPB minimizes the impact of defects up to 1 mm deep on the fatigue life of 17-4 PH H1100 steel by mitigating stress concentration and crack advances in the compressively stressed material, although defects that propagated past this depth had a greater impact on the fatigue propagation and overall lifespan [50]. On the whole, these findings demonstrate that the RSI impact on fatigue propagation largely depends on the magnitude and depth of imparted CRS. Various findings suggest that a critical depth of CRS impingement must be achieved to suppress the fatigue crack growth rate, although considerably more research is needed to analytically understand this value as a function of an alloy's mechanical properties. The magnitude of impact achieved by fatigue initiation and propagation effects may be viewed together through the lens of overall fatigue life.

5.3. Fatigue Life

Consideration of fatigue life combines the fatigue initiation and fatigue crack propagation characteristics of an alloy's performance into a single metric. The effects of RSI treatments on fatigue life are well-known and are typically beneficial, so examples from the literature will be only briefly reviewed across the alloy hardness spectrum. Research on low hardness alloys, RSI, and fatigue life improvement is scarce since these treatments are more often considered for corrosion reduction in these alloys rather than in terms of fatigue. Considering medium-hardness alloys, Takahashi et al. compared SP and LSP treatment effects on fatigue life in 7075-T651 (175 HV) and observed a 7% and 27% improvement at 10^7 cycles, respectively [51]. When notches of various depths were introduced, fatigue propagation testing measured an apparent threshold stress intensity increase of 2 times in the SP specimen and 5 times in the LSP specimen, for which the 3 times deeper residual stress penetration from LSP was considered the cause [51]. Ye et al. demonstrated in 6160-T6 (140 HV) that LSP achieved a CRS as high as 300 MPa in magnitude that decreased to near-zero at 1 mm depth, which increased the fatigue life by 12% at 10^6 cycles [52]. The fatigue improvement was highest in the high-cycle fatigue regime, due to the fatigue initiation on the alloy surface (where CRS was highest), whereas the impact was less measurable in the low-cycle fatigue regime, due to the characteristic defect formation well below the alloy surface at inclusions or other defects [52]. For high-hardness alloys, Fuhr et al. evaluated the SP peening angle and coverage effects on the fatigue strength of Ti-6Al-4V (380 HV) and demonstrated that SP treatment that achieved from 100% to 1200% coverage significantly improved the fatigue strength at 10^7 cycles, with grazing incidence angles surprisingly achieving higher fatigue strengths despite increased surface roughness [53]. Sano et al. evaluated the impact of LSP on 316L stainless steel (220 HV) in rotating bend tests and observed a 1.4–1.7-times increase in fatigue strength compared to untreated 316L, despite the LSP treatment increasing the surface roughness [54] (Figure 5). In DIN 34CrNiMo6 steel (270 HV), alternating bend testing following SP or LPB treatment demonstrated that the fatigue limits increased by 39% and 52%, respectively, following these individual treatments [55]. The difference in performance was due to the greater depth and stability of compressive residual stresses achieved by LPB. Pistochini and Hill achieved a similar result on 300M steel using LSP, with a 54% fatigue life improvement at 10^6 cycles [56]. Similarly, Cherif et al. compared SP, LPB, and UNSM on 304SS (220 HV) and observed the greatest improvement in fatigue life from LPB was due to deeper compressive stress penetration, followed by UNSM and SP, respectively [57].

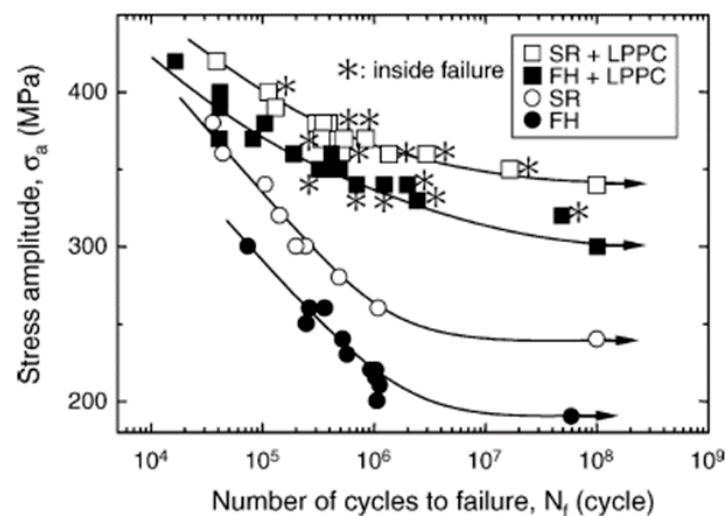


Figure 5. The impact of LSP on 316L fatigue life with stress relief (SR) and without (FH), where LPPC = laser peening with protective coating [54]. Reprinted with permission from [54]. Copyright 2006, Materials Science and Engineering A on behalf of Elsevier.

Altogether, these works demonstrate a strong tendency for RSI to improve fatigue life, which supports the rationale that the mitigation of fatigue propagation overwhelms potential increases in fatigue initiation due to roughness. The magnitudes of fatigue life improvement vary considerably between alloys and specific RSI treatments/settings, and the introduction of corrosive environments further complicates performance prediction. Therefore, expanding upon the background provided regarding the RSI impacts on fatigue in relatively inert environments, the more complex mechanism of corrosion fatigue will be addressed, as will the impacts of RSI on this mechanism.

5.4. Corrosion Fatigue Mitigation

RSI treatments are increasingly utilized in critical applications to reduce the effective tensile stress formed at a stress concentrator, such as a corrosion pit, and to slow fatigue advance by reducing ΔK . When selecting an RSI method for corrosion fatigue mitigation, consideration of the surface roughness and CRS magnitude, as well as penetration depth, become critical due to the increased role of corrosion and the changing surface profile to concentrate stress. In the corrosion fatigue testing of SP 7075-T651 (175 HV) in 0.1 M NaCl, Zupanc and Grum observed a 2-fold corrosion fatigue life improvement by SP, and less pitting occurred on the alloy surface throughout testing, despite the SP sample having similar anodic kinetics in potentiodynamic testing [27]. The fractographic analysis demonstrated that the fatigue initiation preferentially occurred in the subsurface, away from the pits in the SP specimens, suggesting that the CRS mitigated the effective stresses present in the pits [27]. These results agree with those of Lv et al., who demonstrated that SP consistently improved 7050-T7451 (162 HV) corrosion fatigue life, despite increasing amounts of pre-exposure in ASTM G34 EXCO solution and induced pitting damage on the alloy surface [58]. On SAE9354 spring steel (200 HV), Kubota et al. demonstrated a 3.5-fold fatigue life improvement after applying triple-coverage SP treatment, despite the introduction of a 0.25 mm deep artificial pit, and a 1.5-fold improvement was achieved with a 0.50 mm pit (achieved CRS depth of 0.6 mm by the triple SP) [59]. Additionally, Turnbull et al. demonstrated via fatigue testing and modeling on SP 12Cr steel (350 HV) that a 0.25 mm-deep CRS field remains beneficial to improve fatigue life, even after pit growth has penetrated the CRS layer [60,61]. These results were understood through the reduction of stress amplitude and mean stress acting on the crack front, as well as a constraint at the alloy surface affecting the mechanical driving force that acts on the lateral crack fronts, such that the effect of the CRS was measurable on crack growth until the crack depth reached 0.9 mm [60,61].

Moving to UNSM, evaluations of this treatment concerning corrosion fatigue effects largely concern biomedical applications but show promise elsewhere as well. Cao et al. evaluated UNSM Ti-6Al-4V (380 HV) in SBF via potentiodynamic analysis, as well as in fatigue and, despite the UNSM treatment increasing the pitting susceptibility of the alloy, the fatigue life was improved by 10% [38]. Considerable work remains to be done in determining UNSM effects on corrosion fatigue in softer as well as harder alloys. Regarding LSP, Peyre et al. evaluated LSP effects on fatigue in a simulated pit in 2024-T3 (137 HV) and demonstrated a 7-fold fatigue initiation improvement, and 3-fold improvement in fatigue propagation compared to a ground surface [62]. By comparison, the same geometry tested after SP showed a 3-fold improvement during both fatigue initiation and propagation [62]. Luo et al. evaluated single- and double-LSP treatment on 20Cr13 martensitic steel (235 HV) in notched three-point bending tests and measured a roughly 30% and 51% increase in corrosion fatigue life in 0.6 M NaCl [63]. This finding demonstrates that a crack traveling perpendicular to the LSP-treated surfaces was significantly affected by the high magnitude, deep CRS (~2.4 mm depth) on the crack flanks, despite only 32% of the specimen cross-section being in a state of compression [63]. Prev y and Cammett [64] demonstrated on 7075-T6 (175 HV) that LPB was able to impart compressive residual stress to a depth of 1.25 mm in pitted material, which improved the fatigue life by 10 times. Without this treatment, the pitting damage achieved over 500 h in salt fog exposure reduced the fatigue

life by 50% [64]. Similarly, Dzionk et al. found that fretting, as well as pitting corrosion damage, can be overcome through the use of LPB on C35 shaft steel (210 HV) in seawater, achieving a 30% fatigue life improvement overall [65]. These findings demonstrate the robust ability of RSI to improve corrosion fatigue performance in a variety of conditions. Increasingly aggressive service conditions will warrant methods that achieve less roughness and deeper CRS to combat stress concentrations that may be formed at pits or other corrosion sites. The ability to mitigate EAC may also be a consideration under such conditions.

6. Mitigation of Environmentally Assisted Cracking

Environmentally assisted cracking is a common threat to achieving component design life in service, especially as the use of higher-strength alloys becomes increasingly common in aggressive conditions. Despite the diversity of mechanisms that exist that cause EAC, all processes require sufficient applied stress to exceed a threshold stress intensity for a given corrosive environment. When utilizing SP to evaluate hydrogen embrittlement susceptibility in PSB1080 steel (520 HV), Li et al. observed via slow strain rate testing that increasingly intense SP treatment improved the elongation achieved during testing, which is contrary to typical work-hardening behavior [66]. Hydrogen permeation evaluations demonstrated that the dislocation fields induced by the SP reduced hydrogen diffusion into the steel by acting as a hydrogen trap, and the dislocation density increased with the SP intensity [66]. The HE-related crack growth became increasingly branched in the SP test specimens as well. In static bend testing, Brown et al. demonstrated through seacoast exposure that 2014-T651 (155 HV) and 7079-T651 (150 HV) both benefitted from SP treatment, where the residual stress mitigated the onset of SCC failure by 3 months in 2014 and 4+ years in 7079 [67]. In more aggressive alternate immersion settings, by contrast, the SP had a negligible effect in 2014-T651, and extended the alloy life by 4 months in the 7079-T651 [67]. The authors' conclusion from these results was that the characteristically faster pitting rates in 2024-T651 quickly penetrated through the 0.25–0.50 mm compressive surface layer, which greatly decreased the efficacy of the SP in more corrosive conditions [67]. The 7079-T651, by contrast, experienced slower pitting, so that the effect of the SP treatment lasted much longer. These authors also observed that the SP treatment distorted and bent the grain boundaries in the compressive surface layer, which created a more tortuous crack path that slowed crack initiation and the early stages of crack advances [67].

Numerous successful applications of LSP and LPB for EAC mitigation have been published for 316L (220 HV) and 304L (240 HV), for nuclear applications in cooling water environments, such as that shown in Figure 6 [54]. Scheel et al. demonstrated in boiling $MgCl_2$ that the LPB treatment halted EAC in 304L heat-affected zones [68]. Sundar et al. performed similar testing on sensitized 304L and observed increasingly lower EAC susceptibility as the LSP power density was increased from 3.6 GW/cm² to 6.4 GW/cm² [69]. Higher power levels of LSP have also been demonstrated to reduce 304L susceptibility to intergranular corrosion by melting the surface; however, this process may also introduce deleterious tensile stresses and will not be reviewed [31,70].

In AZ31B (83 HV), Zhang et al. demonstrated that LSP reduced the SCC in a NaOH environment through the added CRS and finer surface microstructure [71]. However, studies on brass alloys 260 and 280 (80 HV) demonstrated that LSP treatment mitigated EAC only when certain microstructures/compositions were present (in this case, higher Zn content in brass 280), such that the dezincification was reduced by the added CRS and dislocation densities [72].

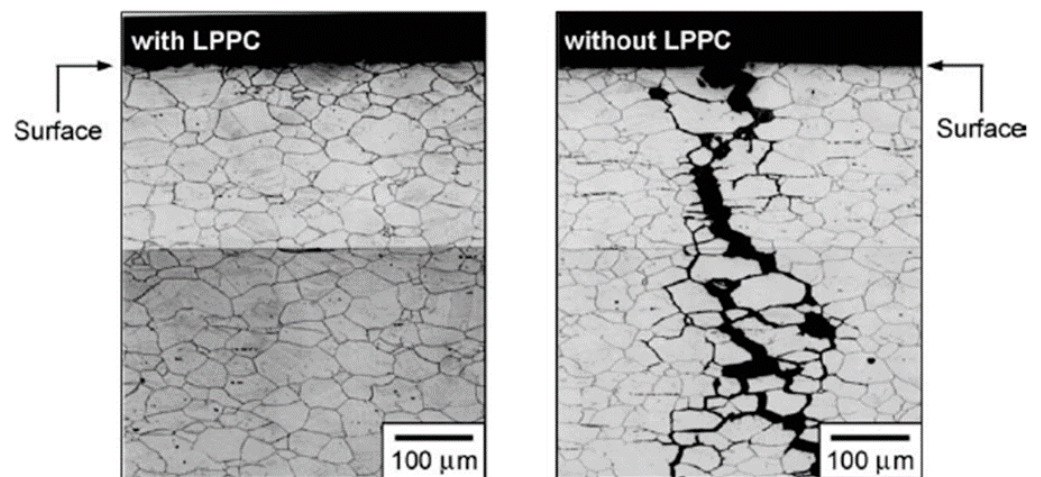


Figure 6. Successful mitigation of stress corrosion cracking in 316L in cooling water due to laser shock peening treatment without an ablative coating [54]. Reprinted with permission from [54]. Copyright 2006, Materials Science and Engineering A on behalf of Elsevier.

Regarding UNSM, Telang et al. utilized this treatment, combined with annealing, to promote special grain boundary junctions in Alloy 600, which reduced the sensitization of the surface and reduced EAC susceptibility in tetrathionate solution [73]. In multi-layered steel, Jo et al. evaluated UNSM treatment for its effect on hydrogen permeability and determined that the 0.2 mm-deep CRS zone created by UNSM acted as a strong hydrogen barrier by storing compressive residual stress, as well as by trapping the hydrogen in the high dislocation densities, twin boundaries, and grain boundaries [74]. These results are in agreement with the SP results from Li et al. [66], demonstrating a consistent capability to reduce hydrogen permeability via RSI treatment to mitigate EAC in the CRS layer. Additionally, Takakuwa et al. demonstrated via modeling that CRS will also reduce hydrogen concentration at an environmental crack tip, by lowering the hydrostatic stress [75]. Altogether, these findings demonstrate that the main means through which RSI treatment may impact EAC susceptibility is:

1. Increased resistance to hydrogen permeability from the treated surface through hydrogen trapping in the CRS zone;
2. Reduced surface corrosion to delay corrosion-related defect formation, stress concentration, and exceeding of the threshold K (K_{TH}); and
3. Reduction of the hydrostatic stress at the crack tip by reducing the resolved tensile stress, which reduces the driving force for hydrogen diffusion into the fracture process zone.

This technical understanding of the effects of RSI on corrosion, corrosion fatigue, and EAC provides substantive background to understand the case studies of successful RSI applications in various industries. Additionally, applied research efforts will be reviewed with an emphasis on potential new uses of RSI technology.

7. Case Studies of RSI Implementation in Industry for Environmental Fracture Mitigation

7.1. Nuclear Industry

Between 1981 and 2011, failure, inspection, and replacement costs incurred due to EAC in nuclear power plant components were estimated to be USD 10 billion [76]. Loss of component integrity in nuclear applications poses a considerable risk due to the sensitivity of operations in power plants, not to mention the difficulty of remaking and replacing large components in critical areas of the plant, such as reactor vessels. EAC in pipework, reactor vessels, and other plant components is often driven by tensile residual stresses from part production, which are ever-present unless balanced by heat treatment or RSI. For this reason, the nuclear power industry has taken a strong interest in LSP to mitigate EAC, as

well as to extend the fatigue life [77]. Toshiba developed and patented an underwater LSP process for treating reactors and other components, with minimal need for plant downtime, and has been utilizing this technique since 1999. An example of such an LSP system design is provided in Figure 7 [8]. This schematic demonstrates the distances that the laser can be transported while still maintaining sufficient power to laser peen high-strength steel components, as well as the complexity of these modern LSP systems. As of 2016, 509 reactors of various types had been treated using Toshiba's LSP process, and none had experienced new instances of SCC in boiling and/or pressurized water applications [77]. A portable LSP system is in development that will further increase the ease of underwater RSI treatment in nuclear and other industrial facilities [78].

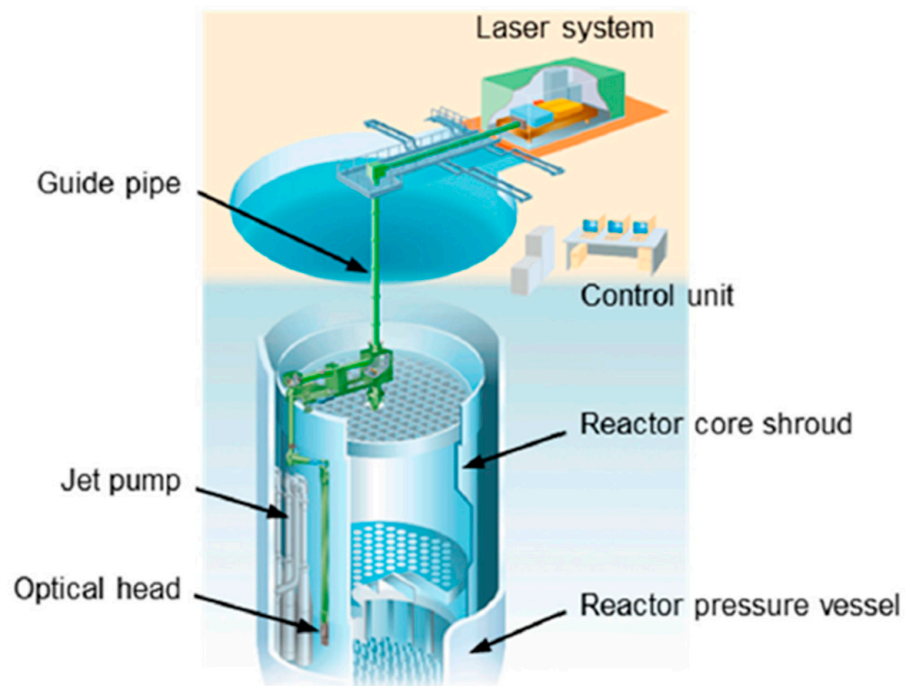


Figure 7. An underwater LSP system design for use in nuclear reactors [8]. Reprinted with permission from [8]. Copyright 2020, Metals journal in MDPI.

Additionally, research on Alloy 718+, utilizing LSP and UNSM, demonstrated that both of these RSI treatments reduced alloy irradiation damage due to the dislocation densities that were introduced, which is an additional source of benefit that may lead to more widespread use of these technologies in the nuclear sector [79]. LPB has potentially adopted a key role in long-term nuclear waste storage by minimizing the EAC susceptibility of closure welds on steel canisters. In 2006, LPB was identified and selected as the favored treatment to prolong the life of closure welds on experimental steel canisters, which was intended to help achieve the 50,000-year life requirement for these containers [80]. The LPB method was utilized in experimental studies as part of the Yucca Mountain long-term nuclear storage program.

7.2. Aerospace Industry

Shot peening has been utilized in the aerospace and other industries for decades but is not always an adequately effective technique due to the shallow CRS depth, as well as the ease of over-treating, both of which raise the risk of unexpected fatigue or fracture in a treated part [81]. The high replicability and deeper CRS achieved by LSP makes this technique more attractive in aerospace applications; for this reason, LSP is now utilized to maintain the F-22 Raptor and the F-35 fighter jets in the United States [82]. In addition to engine blade components, where LSP increases resistance to fatigue, EAC, and

foreign-object damage on leading edges, LSP is also utilized on radar-absorptive materials on the outer body of the F-35, for which maintaining the surface finish is key [83]. Arrestment hooks for aircraft stationed on naval aircraft carriers have high fatigue performance requirements, for which LSP and SP were recently evaluated to promote longer life [84]. This study demonstrated that LSP was more effective at both mitigating crack initiation and extending fatigue life than SP in simulated hook-shank geometries made of Hy-Tuf (474 HV) and Ferrium S53 (589 HV) steel. In commercial aircraft landing gear, which is also made of high-strength steel, fatigue failures have occurred due to high vibratory stresses present when landing and braking, which can cause fast crack growth rates. These failures cumulatively cost Delta Airlines USD 1 million per year in inspection and replacement costs [85]. To remedy this fatigue susceptibility, LPB was utilized to service landing gear in situ during routine maintenance, which mitigated existing crack propagation and stifled new crack initiation. As of 2017, 150 landing-gear components had been LPB-treated on MD-88 aircraft to extend component life [85]. Similar implementation of LPB has been utilized to extend the life of irreplaceable floor beams in the P-3 Orion aircraft fleet, which are prone to fatigue failure at the machined features that produce stress concentration [86].

7.3. Maritime Industry

The maritime industry is estimated to incur USD 2.8 billion in corrosion costs per year, which has created a strong need for coatings and other surface treatments that mitigate environmental damage [87]. One marine part that consistently suffers premature failure issues is propulsion shafting [88,89]. Processes such as SP have been historically used on shafts due to the ease of application on large parts; however, there is interest in more advanced RSI methods that will impart deeper CRS without the same surface finish concerns, since fretting corrosion can initiate corrosion fatigue. Dzionk et al. have developed a system that would enable the simultaneous turning and LPB of the shaft, which would allow consistency of application as well as efficiency [65]. Marine fasteners are also a common failure-point in marine structures, due to corrosion fatigue and EAC. Reggiani and Olmi evaluated SP and LPB in 36NiCrMo and 42CrMoV fasteners (474 HV) for potential fatigue improvement and determined that the smoother surface achieved by the LPB, as well as deeper CRS, led to consistent fatigue life extension, whereas the SP performance depended largely on the intensity and surface roughness [25]. Lastly, Al-Mg alloys (typically 70–80 HV) used in the US Navy fleet have sensitized in service and require considerable maintenance due to EAC, for which a variety of RSI methods are currently in use or may be used in the future to mitigate problems [90]. Ultrasonic impact treatment is currently utilized to mitigate EAC in sensitized Al-Mg, as well as to close active cracks through severe plastic deformation [90]. Development efforts are also underway to create portable LSP systems that could treat a sensitized Al-Mg superstructure [91,92].

7.4. Biomedical Industry

The biomedical industry has an expanding stake in surface treatment technologies, in order to better ensure the long-term integrity and biocompatibility of prostheses, implants, and joining/grafting devices [93]. Mg-based alloys are generating considerable interest due to their stiffness, light weight, similarity to human bone (reduction of stress shielding effects), as well as their overall biocompatibility with the human body [94]. However, Mg-based alloys corrode too quickly, and the rapid generation of hydrogen gas can be problematic. To attempt to address this concern, Uddin et al. evaluated RSI treatments on biodegradable Mg alloys for bone repair and arterial stent applications, in order to regulate the corrosion rate, and theorized that LPB would be a better RSI treatment compared to SP, due to the lower surface roughness, reduced impact on general corrosion susceptibility and CRS that likely exceeds any pitting depth that would occur in Mg implants [95]. Patil found, on the magnesium alloy WE43 (85 HV), that SP increased the corrosion rate in simulated body fluid, due to the increased surface area exposure and roughness associated with increasing the peening pressure, and the corrosion rate increased 2 to 3 times more

when a bending stress was applied, to simulate performance in a potential use case [96]. Cao et al. applied ball-burnishing, a similar method to LPB, to AZ31B (60 HV) to refine the surface microstructure [41]. Immersion for up to 7 days in SBF demonstrated that specific burnishing parameters enabled a mass loss reduction of 64% [41]. Implant alloys can also pose concerns, due to long-term corrosion and the shedding of toxic compositional components, such as chromium. It is known that 316L stainless steel (220 HV), which is a common alloy used in implants, can have these issues over time in SBF. However, Seemikeri et al. successfully demonstrated, via combined experimental and modeling efforts, that LPB could be optimized for 316L in specific conditions in the human body by balancing the surface roughness, hardness, fatigue life, and corrosion/wear properties to reduce such leaching [93]. More research is needed before these technologies will be widely utilized in this sector.

8. Future Needs

This review has discussed a variety of RSI benefits, as well as detriments, to alloy performance, not all of which are fully understood. In terms of corrosion, a common conclusion is that SP, UNSM, and LPB tend to increase the corrosion current density in a variety of alloys, yet LSP tends to slightly improve i_{corr} due to the slight melting and re-segregation caused on the alloy surface. However, long-term testing is scarce in the literature, and examples such as Zupanc and Grum [27] exist on 7075 in 0.1 M NaCl, which demonstrates a reduction in pitting in a corrosive environment when potentiodynamic analysis would suggest that nearly the same pitting susceptibility should occur. Less accelerated evaluations may reveal additional considerations prior to fielding a given RSI method. In terms of corrosion fatigue, a general relationship between the CRS depth and magnitude and the true “breakthrough” pit depth is needed. Since each RSI method entails different levels of costs and infrastructure, such information would be useful to determine the most balanced RSI method and parameter set for a given severity of corrosive service conditions. Lastly, this literature review has demonstrated that a considerable amount of research remains to be done concerning the mitigation of through-crack propagation in RSI-treated components, and a relationship must be found to determine which RSI treatments and CRS magnitudes will reduce the through-thickness crack growth rate for different levels of stress. This information, coupled with an additional evaluation of the relaxation of CRS from each RSI method when applied to common engineering alloys, would enable more accurate fatigue and EAC life predictions when known flaws are present.

9. Conclusions

The present review has focused on SP, UNSM, LSP, and LPB, and the effects of these treatments on corrosion, corrosion fatigue, and EAC in alloys of varying hardness. The literature covering these topics has demonstrated several general trends in RSI performance:

1. Corrosion Mitigation
 - a. RSI performance is highly surface state sensitive, and metallurgy-specific;
 - b. RSI typically increases corrosion current density unless surface melting occurs, however considerably more testing is needed to compare potentiodynamic results with long term corrosion performance;
 - c. Examples exist where RSI treatments mitigate pitting corrosion susceptibility only under certain microstructural conditions, such as prior to sensitization in stainless steel.
2. Corrosion Fatigue Mitigation
 - a. Deeper CRS depth, plus a smooth surface finish, is optimal for improved fatigue performance;
 - b. Increased surface roughness through RSI can increase the likelihood of surface crack initiation under sufficient applied loads;

- c. High CRS magnitude on the surface drives fatigue initiation to below the surface if surface roughness is limited;
 - d. The CRS layer reduces stress concentration caused by corrosion damage to increase the apparent K_{TH} ;
 - e. More research is needed to understand how the crack tip K may continue to be affected by the CRS at depths exceeding the CRS;
 - f. The CRS zone can reduce through-crack propagation in the perpendicular direction, but the relationship between material thickness, CRS zone size, and K is not fully understood.
3. Environmentally Assisted Cracking Mitigation RSI treatment and the CRS layer can mitigate EAC in the following ways:
 - i. By increasing resistance to hydrogen permeability from the treated surface through hydrogen trapping in the CRS zone;
 - ii. By reducing surface corrosion to delay corrosion-related defect formation, stress concentration, and exceedance of K_{TH} ; and
 - iii. By reducing the hydrostatic stress at the crack tip and reducing the resolved tensile stress, which decreases the driving force for hydrogen diffusion into the fracture process zone.

The numerous examples of trends in performance for a given RSI method, as well as the encountered counterexamples, support the need to experimentally evaluate any given RSI treatment and specific settings on the alloy of interest, prior to full-scale deployment.

Funding: This research received no external funding.

Institutional Review Board Statement: Not applicable.

Informed Consent Statement: Not applicable.

Data Availability Statement: No original data were reported in this review.

Conflicts of Interest: The author declares no conflict of interest.

References

1. Anderson, T.L. *Fracture Mechanics: Fundamentals and Applications*, 4th ed.; CRC Press: Boca Raton, FL, USA, 2017; pp. 471–578.
2. Shih, C.F.; DeLorenzi, H.G.; Andrews, W.R. Studies on crack initiation and stable crack growth. In *Elastic-Plastic Fracture*; ASTM International: West Conshohocken, PA, USA, 2009; pp. 65–120. [[CrossRef](#)]
3. McClung, R.C. A literature survey on the stability and significance of residual stresses during fatigue. *Fatigue Fract. Eng. Mater. Struct.* **2007**, *30*, 173–205. [[CrossRef](#)]
4. Schulze, V. *Modern Mechanical Surface Treatment: States, Stability, Effects*; Wiley-VCH: Weinheim, Germany, 2005; pp. 60–350.
5. Lu, J. (Ed.) *Handbook on Residual Stress*, 2nd ed.; Society for Experimental Mechanics: Bethel, CT, USA, 2005; pp. 30–50.
6. Montross, C.S. Laser shock processing and its effects on microstructure and properties of metal alloys: A review. *Int. J. Fatigue* **2002**, *24*, 1021–1036. [[CrossRef](#)]
7. Sundar, R.; Ganesh, P.; Gupta, R.K.; Ragvendra, G.; Pant, B.K.; Kain, V.; Ranganathan, K.; Kaul, R.; Bindra, K.S. Laser Shock Peening and its Applications: A Review. *Lasers Manuf. Mater. Process.* **2019**, *6*, 424–463. [[CrossRef](#)]
8. Sano, Y. Quarter Century Development of Laser Peening without Coating. *Metals* **2020**, *10*, 152–163. [[CrossRef](#)]
9. Priyadarsini, C.; Ramana, V.V.; Prabha, K.A.; Swetha, S. A Review on Ball, Roller, Low Plasticity Burnishing Process. *Mater. Today Proc.* **2019**, *18*, 5087–5099. [[CrossRef](#)]
10. Maamoun, A.H.; Elbestawi, M.A.; Veldhuis, S.C. Influence of Shot Peening on AlSi10Mg Parts Fabricated by Additive Manufacturing. *J. Manuf. Mater. Process.* **2018**, *2*, 40. [[CrossRef](#)]
11. Al-Obaid, Y.F. A Rudimentary Analysis of Improving Fatigue Life of Metals by Shot-Peening. *J. Appl. Mech.* **1990**, *57*, 307–312. [[CrossRef](#)]
12. Maleki, E.; Unal, O.; Guagliano, M.; Bagherifard, S. The effects of shot peening, laser shock peening and ultrasonic nanocrystal surface modification on the fatigue strength of Inconel 718. *Mater. Sci. Eng. A* **2021**, *810*, 141029–141040. [[CrossRef](#)]
13. Zhuang, W.; Liu, Q.; Djugum, R.; Sharp, P.; Paradowska, A. Deep surface rolling for fatigue life enhancement of laser clad aircraft aluminium alloy. *Appl. Surf. Sci.* **2014**, *320*, 558–562. [[CrossRef](#)]
14. Ferreira, N.; Antunes, P.V.; Ferreira, J.A.M.; Costa, J.; Capela, C. Effects of Shot-Peening and Stress Ratio on the Fatigue Crack Propagation of AL 7475-T7351 Specimens. *Appl. Sci.* **2018**, *8*, 375. [[CrossRef](#)]

15. Gujba, A.K.; Medraj, M. Laser Peening Process and Its Impact on Materials Properties in Comparison with Shot Peening and Ultrasonic Impact Peening. *Materials* **2014**, *7*, 7925–7974. [[CrossRef](#)] [[PubMed](#)]
16. Amanov, A.; Pyun, Y. A comprehensive review of nanostructured materials by ultrasonic nanocrystal surface modification technique. *J. Eng.* **2015**, *2015*, 144–149. [[CrossRef](#)]
17. González, J.A.P.; Gomez-Rosas, G.; Ocaña, J.L.; Molpeceres, C.; Banderas, A.; Porro, J.; Morales, M. Effect of an absorbent overlay on the residual stress field induced by laser shock processing on aluminum samples. *Appl. Surf. Sci.* **2006**, *252*, 6201–6205. [[CrossRef](#)]
18. Trdan, U.; Grum, J. Investigation of Corrosion Behaviour of Aluminium Alloy Subjected to Laser Shock Peening without a Protective Coating. *Adv. Mater. Sci. Eng.* **2015**, *2015*, 705306. [[CrossRef](#)]
19. Trdan, U.; Grum, J. Evaluation of corrosion resistance of AA6082-T651 aluminium alloy after laser shock peening by means of cyclic polarisation and EIS methods. *Corros. Sci.* **2012**, *59*, 324–333. [[CrossRef](#)]
20. Sticchi, M.; Schnubel, D.; Kashaev, N.; Huber, N. Review of Residual Stress Modification Techniques for Extending the Fatigue Life of Metallic Aircraft Components. *Appl. Mech. Rev.* **2014**, *67*, 010801. [[CrossRef](#)]
21. Zhuang, W.; Wicks, B. Mechanical Surface Treatment Technologies for Gas Turbine Engine Components. *J. Eng. Gas. Turbines Power* **2003**, *125*, 1021–1025. [[CrossRef](#)]
22. Evgeny, B.; Hughes, T.; Eskin, D. Effect of surface roughness on corrosion behaviour of low carbon steel in inhibited 4 M hydrochloric acid under laminar and turbulent flow conditions. *Corros. Sci.* **2016**, *103*, 196–205. [[CrossRef](#)]
23. Sohrabi, M.J.; Mirzadeh, H.; Dehghanian, C. Unraveling the effects of surface preparation on the pitting corrosion resistance of austenitic stainless steel. *Arch. Civ. Mech. Eng.* **2020**, *20*, 8. [[CrossRef](#)]
24. Trung, P.Q.; Khun, N.W.; Butler, D.L. Effect of Shot Peening Process on the Fatigue Life of Shot Peened Low Alloy Steel. *J. Eng. Mater. Technol.* **2017**, *140*, 011013. [[CrossRef](#)]
25. Reggiani, B. Experimental Investigation on the Effect of Shot Peening and Deep Rolling on the Fatigue Response of High Strength Fasteners. *Metals* **2019**, *9*, 1093. [[CrossRef](#)]
26. Curtis, S.A.; Rios, E.R.D.L.; Rodopoulos, C.A.; Romero, J.S.; Levers, A. Investigating the Benefits of Controlled Shot Peening on Corrosion Fatigue of Aluminium Alloy 2024 T351. In *Shot Peening*; Wagner, L., Ed.; Wiley-VCH Verlag GmbH & Co. KGaA: Weinheim, Germany, 2003; pp. 264–270. [[CrossRef](#)]
27. Zupanc, U.; Grum, J. Effect of pitting corrosion on fatigue performance of shot-peened aluminium alloy 7075-T651. *J. Mater. Process. Technol.* **2010**, *210*, 1197–1202. [[CrossRef](#)]
28. Peltz, J.D.S.; Beltrami, L.V.R.; Kunst, S.R.; Brandolt, C.; Malfatti, C.D.F. Effect of the Shot Peening Process on the Corrosion and Oxidation Resistance of AISI430 Stainless Steel. *Mater. Res.* **2015**, *18*, 538–545. [[CrossRef](#)]
29. Iswanto, P.T.; Malau, V.; Priyambodo, B.H.; Wibowo, T.N.; Amin, N. Effect of Shot-Peening on Hardness and Pitting Corrosion Rate on Load-Bearing Implant Material AISI 304. *Mater. Sci. Forum* **2017**, *901*, 91–96. [[CrossRef](#)]
30. Peyre, P.; Scherpereel, X.; Berthe, L.; Carboni, C.; Fabbro, R.; Béranger, G.; Lemaitre, C. Surface modifications induced in 316L steel by laser peening and shot-peening. Influence on pitting corrosion resistance. *Mater. Sci. Eng. A* **2000**, *280*, 294–302. [[CrossRef](#)]
31. Yue, T.M.; Yan, L.; Chan, C. Stress corrosion cracking behavior of Nd:YAG laser-treated aluminum alloy 7075. *Appl. Surf. Sci.* **2006**, *252*, 5026–5034. [[CrossRef](#)]
32. Ciuffini, A.F.; Barella, S.; Martínez, L.B.P.; Mapelli, C.; Pariente, I.F. Influence of Microstructure and Shot Peening Treatment on Corrosion Resistance of AISI F55-UNS S32760 Super Duplex Stainless Steel. *Materials* **2018**, *11*, 1038. [[CrossRef](#)] [[PubMed](#)]
33. Hou, X.; Qin, H.; Gao, H.; Mankoci, S.; Zhang, R.; Zhou, X.; Ren, Z.; Doll, G.L.; Martini, A.; Sahai, N.; et al. A systematic study of mechanical properties, corrosion behavior and biocompatibility of AZ31B Mg alloy after ultrasonic nanocrystal surface modification. *Mater. Sci. Eng. C* **2017**, *78*, 1061–1071. [[CrossRef](#)]
34. Kim, K.T.; Kim, Y.S. Effect of the Amplitude in Ultrasonic Nano-crystalline Surface Modification on the Corrosion Properties of Alloy 600. *Corr. Sci. Tech.* **2019**, *18*, 196–205. [[CrossRef](#)]
35. Ren, Z.; Hou, X.; Dong, Y.; Ye, C. Effect of Nanocrystallization-Assisted Nitriding on the Corrosion Behavior of AISI 4140 Steel. In Proceedings of the ASME 2016 11th International Manufacturing Science and Engineering Conference, Blacksburg, VA, USA, 27 June 27–1 July 2016; 2016; Volume 49903, p. V002T01A008. [[CrossRef](#)]
36. Li, S.; Ren, Z.; Dong, Y.; Ye, C.; Cheng, G.; Cong, H. Enhanced Pitting Corrosion Resistance of 304 SS in 3.5 wt% NaCl by Ultrasonic Nanocrystal Surface Modification. *J. Electrochem. Soc.* **2017**, *164*, C682–C689. [[CrossRef](#)]
37. Kim, K.-T.; Lee, J.-H.; Kim, Y.-S. Effect of Ultrasonic Nano-Crystal Surface Modification (UNSM) on the Passivation Behavior of Aged 316L Stainless Steel. *Materials* **2017**, *10*, 713. [[CrossRef](#)] [[PubMed](#)]
38. Cao, X.; Xu, X.; Wang, C.; Pyoun, Y.; Wang, Q. Effect of Ultrasonic Surface Impact on the Fatigue Behavior of Ti-6Al-4V Subject to Simulated Body Fluid. *Metals* **2017**, *7*, 440. [[CrossRef](#)]
39. Yang, Y.; Zhou, W.; Tong, Z.; Chen, L.; Yang, X.; Larson, E.A.; Ren, X. Electrochemical Corrosion Behavior of 5083 Aluminum Alloy Subjected to Laser Shock Peening. *J. Mater. Eng. Perform.* **2019**, *28*, 6081–6091. [[CrossRef](#)]
40. Aravamudhan, B.H. Study of the Effect of Laser Shock Peening on Corrosion Behavior of Aluminum Alloy 7075. Master's Thesis, Department Mechanical and Materials Engineering, University of Cincinnati, Cincinnati, OH, USA, July 2018.
41. Cao, C.; Zhu, J.; Tanaka, T.; Pham, D.N. Investigation of Corrosion Resistance Enhancement for Biodegradable Magnesium Alloy by Ball Burnishing Process. *Int. J. Autom. Technol.* **2020**, *14*, 175–183. [[CrossRef](#)]
42. Gangaraj, S.M.H. Side effects of shot peening on fatigue crack initiation life. *Int. J. Eng.* **2011**, 275–280. [[CrossRef](#)]

43. Wagner, L. Mechanical surface treatments on titanium, aluminum and magnesium alloys. *Mater. Sci. Eng. A* **1999**, *263*, 210–216. [[CrossRef](#)]
44. Bag, A.; Delbergue, D.; Ajaja, J.; Bocher, P.; Lévesque, M.; Brochu, M. Effect of different shot peening conditions on the fatigue life of 300 M steel submitted to high stress amplitudes. *Int. J. Fatigue* **2019**, *130*, 105274–105286. [[CrossRef](#)]
45. Wang, Y.; Zhang, Y.; Song, G.; Niu, W.; Xu, Z.; Huang, C. Effect of shot peening on fatigue crack propagation of Ti6Al4V. *Mater. Today Commun.* **2020**, *25*, 101430–101438. [[CrossRef](#)]
46. Hatamleh, O.; Lyons, J.; Forman, R. Laser and shot peening effects on fatigue crack growth in friction stir welded 7075-T7351 aluminum alloy joints. *Int. J. Fatigue* **2007**, *29*, 421–434. [[CrossRef](#)]
47. Hu, Y.; Cheng, H.; Yu, J.; Yao, Z. An experimental study on crack closure induced by laser peening in pre-cracked aluminum alloy 2024-T351 and fatigue life extension. *Int. J. Fatigue* **2019**, *130*, 105232–105242. [[CrossRef](#)]
48. Kashaei, N.; Ventzke, V.; Horstmann, M.; Chupakhin, S.; Riekehr, S.; Falck, R.; Maawad, E.; Staron, P.; Schell, N.; Huber, N. Effects of laser shock peening on the microstructure and fatigue crack propagation behaviour of thin AA2024 specimens. *Int. J. Fatigue* **2017**, *98*, 223–233. [[CrossRef](#)]
49. Huang, S.; Zhou, J.; Sheng, J.; Lu, J.; Sun, G.; Meng, X.; Zuo, L.; Ruan, H.; Chen, H. Effects of laser energy on fatigue crack growth properties of 6061-T6 aluminum alloy subjected to multiple laser peening. *Eng. Fract. Mech.* **2013**, *99*, 87–100. [[CrossRef](#)]
50. Prevey, P.S.; Jayaraman, N.; Ravindranath, R. Low plasticity burnishing treatment to mitigate FOD and corrosion fatigue damage in 17-4 PH stainless steel. In Proceedings of the 2003 Tri-Service Corrosion Conference, Las Vegas, NV, USA, 17–21 November 2003.
51. Takahashi, K.; Kogishi, Y.; Shibuya, N.; Kumeno, F. Effects of laser peening on the fatigue strength and defect tolerance of aluminum alloy. *Fatigue Fract. Eng. Mater. Struct.* **2020**, *43*, 845–856. [[CrossRef](#)]
52. Ye, C.; Liao, Y.; Cheng, G.J. Warm Laser Shock Peening Driven Nanostructures and Their Effects on Fatigue Performance in Aluminium Alloy 6160. *Adv. Eng. Mater.* **2010**, *12*, 291–297. [[CrossRef](#)]
53. Fuhr, J.P.; Basha, M.; Wollmann, M.; Wagner, L. Coverage and Peening Angle Effects in Shot Peening on HCF Performance of Ti-6Al-4V. *Procedia Eng.* **2018**, *213*, 682–690. [[CrossRef](#)]
54. Sano, Y.; Obata, M.; Kubo, T.; Mukai, N.; Yoda, M.; Masaki, K.; Ochi, Y. Retardation of crack initiation and growth in austenitic stainless steels by laser peening without protective coating. *Mater. Sci. Eng. A* **2006**, *417*, 334–340. [[CrossRef](#)]
55. Avilés, A.; Avilés, R.; Albizuri, J.; Pallarés-Santasmartas, L.; Rodríguez, A. Effect of shot-peening and low-plasticity burnishing on the high-cycle fatigue strength of DIN 34CrNiMo6 alloy steel. *Int. J. Fatigue* **2018**, *119*, 338–354. [[CrossRef](#)]
56. Pistochini, T.; Hill, M.R. Effect of laser peening on fatigue performance in 300M steel. *Fatigue Fract. Eng. Mater. Struct.* **2011**, *34*, 521–533. [[CrossRef](#)]
57. Cherif, A.; Pyoun, Y.; Scholtes, B. Effects of Ultrasonic Nanocrystal Surface Modification (UNSM) on Residual Stress State and Fatigue Strength of AISI 304. *J. Mater. Eng. Perform.* **2009**, *19*, 282–286. [[CrossRef](#)]
58. Sheng-Li, L.; Cui, Y.; Gao, X.; Srivatsan, T. Influence of exposure to aggressive environment on fatigue behavior of a shot peened high strength aluminum alloy. *Mater. Sci. Eng. A* **2013**, *574*, 243–252. [[CrossRef](#)]
59. Kubota, M.; Suzuki, T.; Hirakami, D.; Ushioda, K. Influence of Hydrogen on Fatigue Property of Suspension Spring Steel with Artificial Corrosion Pit after Multi-step Shot Peening. *ISIJ Int.* **2015**, *55*, 2667–2676. [[CrossRef](#)]
60. Turnbull, A.; Zhou, S. Impact of pitting corrosion on the benefit of shot peening. In Proceedings of the NACE Corrosion 2018 Proceedings, Paper No. 10630, Phoenix, AZ, USA, 15–19 April 2018.
61. Turnbull, A.; Crocker, L.; Zhou, S. Do corrosion pits eliminate the benefit of shot-peening? *Int. J. Fatigue* **2018**, *116*, 439–447. [[CrossRef](#)]
62. Peyre, P.; Fabbro, R.; Merrien, P.; Lieurade, H.P. Laser shock processing of aluminum alloys: Application to high cycle fatigue behavior. *Mat. Sci. Eng.* **1996**, *A210*, 102–113. [[CrossRef](#)]
63. Luo, K.; Yin, Y.; Wang, C.; Chai, Q.; Cai, J.; Lu, J.; Lu, Y. Effects of laser shock peening with different coverage layers on fatigue behaviour and fractural morphology of Fe-Cr alloy in NaCl solution. *J. Alloys Compd.* **2018**, *773*, 168–179. [[CrossRef](#)]
64. Prevey, P.S.; Cammett, J.; Prevéy, P.S. Low Cost Corrosion Damage Mitigation and Improved Fatigue Performance of Low Plasticity Burnished 7075-T6. *J. Mater. Eng. Perform.* **2001**, *10*, 548–555. [[CrossRef](#)]
65. Dzionk, S.; Przybylski, W.; Ścibiorski, B. The Possibilities of Improving the Fatigue Durability of the Ship Propeller Shaft by Burnishing Process. *Machines* **2020**, *8*, 63. [[CrossRef](#)]
66. Li, X.; Zhang, J.; Wang, Y.; Ma, M.; Shen, S.; Song, X. The dual role of shot peening in hydrogen-assisted cracking of PSB1080 high strength steel. *Mater. Des.* **2016**, *110*, 602–615. [[CrossRef](#)]
67. Brown, B.F. *Stress Corrosion Cracking in High Strength Steels and in Titanium and Aluminum Alloys*; Naval Research Laboratory: Washington, DC, USA, 1972; p. A030873.
68. Scheel, J.E.; Hornbach, D.J.; Prevey, P.S. Mitigation of stress corrosion cracking in nuclear weldments using low plasticity burnishing. In Proceedings of the 16th International Conference on Nuclear Engineering, Orlando, FL, USA, 11–15 May 2008.
69. Sundar, R.; Ganesh, P.; Kumar, B.S.; Gupta, R.K.; Nagpure, D.C.; Kaul, R.; Ranganathan, K.; Bindra, K.S.; Kain, V.; Oak, S.M.; et al. Mitigation of Stress Corrosion Cracking Susceptibility of Machined 304L Stainless Steel Through Laser Peening. *J. Mater. Eng. Perform.* **2016**, *25*, 3710–3724. [[CrossRef](#)]

70. Gupta, R.K.; Sundar, R.; Kumar, B.S.; Ganesh, P.; Kaul, R.; Ranganathan, K.; Bindra, K.S.; Kain, V.; Oak, S.M.; Kukreja, L.M. A Hybrid Laser Surface Treatment for Refurbishment of Stress Corrosion Cracking Damaged 304L Stainless Steel. *J. Mater. Eng. Perform.* **2015**, *24*, 2569–2576. [CrossRef]
71. Zhang, L.-J.; Zhang, H.-B.; Lei, X.-W.; Wang, R.; Han, B.-F.; Zhang, J.-X.; Na, S.-J. Laser processing of Mg-10Li-3Al-3Zn alloy: Part II- Improving corrosion resistance of multi-phase Mg alloys by laser surface processing. *J. Manuf. Process.* **2020**, *56*, 571–580. [CrossRef]
72. Lisenko, N.; Evans, C.D.; Yao, Y.L. Effect of brass composition and phases on stress corrosion mitigation by laser shock peening. *Manuf. Lett.* **2019**, *23*, 5–8. [CrossRef]
73. Telang, A.; Gill, A.S.; Tammana, D.; Wen, X.; Kumar, M.; Teyseyre, S.; Mannava, S.R.; Qian, D.; Vasudevan, V.K. Surface grain boundary engineering of Alloy 600 for improved resistance to stress corrosion cracking. *Mater. Sci. Eng. A* **2015**, *648*, 280–288. [CrossRef]
74. Jo, M.C.; Yoo, J.; Amanov, A.; Song, T.; Kim, S.-H.; Sohn, S.S.; Lee, S. Ultrasonic nanocrystal surface modification for strength improvement and suppression of hydrogen permeation in multi-layered steel. *J. Alloys Compd.* **2021**, *885*, 160975–160985. [CrossRef]
75. Takakuwa, O.; Nishikawa, M.; Soyama, H. Numerical simulation of the effects of residual stress on the concentration of hydrogen around a crack tip. *Surf. Coat. Technol.* **2012**, *206*, 2892–2898. [CrossRef]
76. Scheel, J.E.; Jayaraman, N.; Hornbach, D.J. Engineered Residual Stress to Mitigate Stress Corrosion Cracking of Stainless Steel Weldments. In Proceedings of the NACE Corrosion 2011, NACE-11283, Houston, TX, USA, 13–17 March 2011.
77. Westinghouse Electric Company. The Art of Aging Well: Westinghouse Introduces Laser Peening. 1 October 2017. Available online: <https://info.westinghousenuclear.com/blog/the-art-of-aging-well-westinghouse-introduces-laser-peening> (accessed on 4 October 2021).
78. Uehara, T.; Yoda, M.; Sano, Y.; Mukai, N.; Chida, I.; Kato, H. Laser peening systems for preventive maintenance against stress corrosion cracking in nuclear power reactors. In Proceedings of the International Conference on Nuclear Engineering, Orlando, FL, USA, 11–15 May 2008; Volume 48140, pp. 491–497.
79. Bazarbayev, Y.; Kattoura, M.; Mao, K.S.; Song, J.; Vasudevan, V.K.; Wharry, J.P. Effects of corrosion-inhibiting surface treatments on irradiated microstructure development in Ni-base alloy 718. *J. Nucl. Mater.* **2018**, *512*, 276–287. [CrossRef]
80. Prevey, J. Lambda Technologies Keeps Nuclear Waste Materials Contained. 30 October 2018. Available online: https://www.prweb.com/releases/lambda_technologies_keeps_nuclear_waste_materials_contained/prweb15879924.htm (accessed on 24 April 2021).
81. Scheel, J.E.; Prevey, P.S.; Hornbach, D.J. The effect of surface enhancement on the corrosion properties, fatigue strength, and degradation of aircraft aluminum. In Proceedings of the NACE Corrosion 2010, Paper No. 10087, San Antonio, TX, USA, 14–18 March 2010.
82. Naval Air Systems Command. New F-35 Modification Facility Brings Strategic Capability to FRCE. 20 August 2019. Available online: <https://www.navair.navy.mil/news/New-F-35-modification-facility-brings-strategic-capability-FRCE/Tue-08202019-0732> (accessed on 22 April 2021).
83. Zabeen, S.; Preuss, M.; Withers, P. Evolution of a laser shock peened residual stress field locally with foreign object damage and subsequent fatigue crack growth. *Acta Mater.* **2015**, *83*, 216–226. [CrossRef]
84. Leap, M.; Rankin, J.; Harrison, J.; Hackel, L.; Nemeth, J.; Candela, J. Effects of laser peening on fatigue life in an arrestment hook shank application for Naval aircraft. *Int. J. Fatigue* **2011**, *33*, 788–799. [CrossRef]
85. Lambda Technologies Group. Landing Gear. 2017. Available online: https://www.lambdatechs.com/wp-content/uploads/LandingGear_v2.pdf (accessed on 10 April 2021).
86. Lambda Technologies Group. Improving Component Life and Performance: Aircraft Structures. 2011. Available online: <https://www.lambdatechs.com/wp-content/uploads/AircraftStructures.pdf> (accessed on 10 April 2021).
87. NACE. Corrosion Costs and Preventative Strategies in the United States. Available online: <http://impact.nace.org/documents/ccsupp.pdf> (accessed on 15 August 2021).
88. Zapffe, C.A. Corrosion-Fatigue Failure of a Marine Propeller Shaft. *Corrosion* **1953**, *9*, 298–302. [CrossRef]
89. Hara, S. The Corrosion Fatigue of Marine Propeller Shaft. *J. Zosen Kiokai* **1955**, *1955*, 135–148. [CrossRef]
90. Golumbskie, W.; Tran, K.; Noland, J.; Park, R.; Stiles, D.; Grogan, G.; Wong, C. Survey of Detection, Mitigation, and Repair Technologies to Address Problems Caused by Sensitization of Al-Mg Alloys on Navy Ships. *Corrosion* **2016**, *72*, 314–328. [CrossRef]
91. Onboard Ship Integration of Laser Peening System for Lasting Aluminum Repairs. NSRP. Available online: <https://www.nsrp.org/project/onboard-ship-integration-of-laser-peening-system-for-lasting-aluminum-repairs/> (accessed on 28 December 2020).
92. Hackel, L.A.; Dane, C.B.; Harris, F.B.; Rankin, J.; Truong, C. Transportable Laser Peening System for Field Applications to Improve Fatigue and SCC Resistance of Offshore Components and Structures. In Proceedings of the Sixteenth International Offshore and Polar Engineering Conference, San Francisco, CA, USA, 28 May–2 June 2006; pp. 193–198. [CrossRef]
93. Seemikeri, C.Y.; Brahmkar, P.K.; Mahagaonkar, S.B. Low Plasticity Burnishing: An Innovative Manufacturing Method for Biomedical Applications. *J. Manuf. Sci. Eng.* **2008**, *130*, 021008–021016. [CrossRef]
94. Russo, J. The Effects of Laser Shock Peening on the Residual Stress and Corrosion Characteristics of Magnesium Alloy AZ91D for Use as Biodegradable Implants. Master’s Thesis, School of Dynamic Systems, University of Cincinnati, Cincinnati, OH, USA, 2012.

-
95. Uddin, M.S.; Hall, C.; Murphy, P. Surface treatments for controlling corrosion rate of biodegradable Mg and Mg-based alloy implants. *Sci. Technol. Adv. Mater.* **2015**, *16*, 053501–053525. [[CrossRef](#)]
 96. Patil, T. Effect of Shot Peening on Stress Corrosion Behavior of Biodegradable Magnesium WE43. Master's Thesis, University of Nebraska Graduate College, Lincoln, NE, USA, April 2018.